Original Paper

Dissolution behaviour of biosoluble HT stone wool fibres

Thomas Steenberg, Helene Kähler Hjenner, Søren Lund Jensen, Marianne Guldberg and Torben Knudsen

Rockwool International A/S, Hedehusene (Denmark)

The dissolution behaviour of two types of fibres, the biosoluble HT and the traditional MMVF21 stone wool fibres, in synthetic simulated lung fluid (Gamble's solution) at pH 4.5 was investigated in order to clarify the mechanisms, and the effect of the various constituents in the liquid.

The Gamble's solution contains various organic acids and salts. The study showed that organic acids which are able to form complexes with aluminium (e.g. citric and tartaric acid) caused both fibres to dissolve at a high rate at pH 4.5. Organic acids without the ability to form complexes with aluminium (e.g. acetic, maleic, lactic and pyruvatic acid) have no (or minor) impact on the dissolution rate at pH 4.5.

The presence of sodium chloride lowers the dissolution rate, especially that of MMVF21. The silica that remains when the silica network has been depleted of aluminium ions (due to citric and tartaric acid) behaves differently in the two fibres. In HT fibres the silica dissolves at a high rate, probably as a diluted sol. Thus the HT fibre has a high dissolution rate in Gamble's solution at pH 4.5. For the MMVF21 fibre, condensation of the silica network as a gel results in a lower dissolution rate. It is assumed that the different Al/(Al+Si) ratios for HT and MMVF21 fibres explain why the fibres behave differently.

Auflösungsverhalten von biolöslichen HT-Steinwollefasern

Das Auflösungsverhalten zweier Fasertypen, der biolöslichen HT- und der herkömmlichen MMVF21-Steinwollefasern, wurde in synthetischer simulierter Lungenflüssigkeit (Gamble-Lösung) bei einem pH-Wert von 4,5 untersucht, um die Mechanismen und den Einfluß der unterschiedlichen Komponenten in der Flüssigkeit zu klären.

Die Gamble-Lösung enthält verschiedene organische Säuren und Salze. Die Untersuchung zeigte, daß organische Säuren, die mit Aluminium Komplexe bilden können (z.B. Zitronen- und Weinsäure), bei einem pH-Wert von 4,5 eine sehr schnelle Auflösung beider Fasern bewirken. Organische Säuren, die nicht die Fähigkeit besitzen, mit Aluminium Komplexe zu bilden (z.B. Essig-, Malein-, Milch- und Brenztraubensäure), haben keine oder nur eine geringe Auswirkung auf die Auflösungsrate bei einem pH-Wert von 4,5.

Die Anwesenheit von Natriumchlorid verringert die Auflösungsrate, besonders die der MMVF21-Faser. Wenn die Aluminium-Ionen aus dem SiO_2-Netzwerk herausgelöst sind (durch Zitronen- und Weinsäure), verhält sich das verbleibende SiO_2 der beiden Fasern unterschiedlich. In den HT-Fasern löst sich das Siliciumdioxid sehr schnell auf, wahrscheinlich wie ein verdünntes Sol. Daher hat die HT-Faser eine hohe Auflösungsrate in der Gamble-Lösung bei einem pH-Wert von 4.5. Bei der MMVF21-Faser führt die Verdichtung des SiO_2-Netzwerkes zu einem Gel mit einer niedrigeren Auflösungsrate. Es wird angenommen, daß die unterschiedlichen Al/(Al+Si)-Verhältnisse von HT- und MMVF21-Fasern die Erklärung dafür sind, daß die Fasern sich unterschiedlich verhalten.

1. Introduction

The potential pathogenicity of a given fibre type is mainly dependent upon the extent to which the fibres can be inhaled and can persist in the lung [1]. In the lung at least two pH environments exist which influence the degradation of the fibres [2]: pH 7.4 (the extra-cellular environment) and pH 4.5 to 5 (the environment found within the phagolysosomes of the macrophages).

A number of in-vitro dissolution measurements in artificial lung fluids at near-neutral pH ($\approx$ 7.4) and at acidic pH ($\approx$ 4.5) have been performed to simulate the dissolution processes occurring in vivo [3 to 10]. For some MMVFs the in-vitro dissolution rate at pH 7.4 can be correlated to the results of in-vivo studies [11], whereas for other fibres the dissolution rate at pH 4.5 has to be taken into account [10, 12 to 14]. The biosoluble high alumina–low silica HT stone wool fibres (CAS no. 287922-11-6) belong to the latter category [14 and 15].

The in-vitro dissolution rate at pH 4.5 of HT fibres is approximately ten times higher than that of traditional stone wool fibres [15], when measured according to e.g. the guidelines developed by the European Insulation Manufacturers Association, Brussels (Belgium) [16]. However, the measured dissolution rates have proven

Received 19 January, revised manuscript 21 March 2001.

Table 1. Chemical composition (in w%) of the HT fibre and the traditional stone wool fibre (MMVF21). Fibres with a slightly modified (suffix: mod) chemical composition are used for the optical setup. The fibres are without oil and binder.

fibre type	SiO_2	Al_2O_3	TiO_2	FeO	CaO	MgO	Na_2O	K_2O	P_2O_5
HT	38.7	22.0	1.9	7.2	14.9	10.1	1.8	0.8	0.4
MMVF21	46.1	13.2	2.8	6.3	16.6	9.3	2.6	1.3	<0.1
HT_{mod}	40.6	20.8	1.6	7.1	13.6	11.4	1.6	0.8	0.3
$MMVF21_{mod}$	45.8	14.9	1.6	7.6	14.3	10.9	2.0	1.0	0.4

Table 2. Chemical composition of the modified Gamble's solution (synthetic simulated lung fluid) [16]. HCl was added to achieve pH 4.5.

compound	concentration in mmol/l
$NaHCO_3$	23.2
NaCl	121.8
$MgCl_2 \cdot 6H_2O$	1.0
$CaCl_2 \cdot 2H_2O$	0.2
Na_2HPO_4	1.0
Na_2SO_4	0.6
$H_2NCH_2CO_2H$ (glycine)	1.6
$HOC(CH_2CO_2Na)_2CO_2Na \cdot 2H_2O$ (sodium citrate)	0.52
$NaO_2CCH(OH)CH(OH)CO_2Na \cdot 2H_2O$ (sodium tartrate)	0.8
CH_3COCO_2Na (sodium pyruvate)	1.6
$CH_3CH(OH)CO_2H$ (lactic acid)	1.7

very sensitive to the test conditions, especially the flow-rate/surface area ratio and the organic acids present in the synthetic lung fluid [9, 10 and 12]. The dissolution rate of HT fibres at pH 7.4 is much lower than the dissolution rate at pH 4.5, and only slightly higher than that of traditional stone wool fibres at pH 7.4 [10 and 12]. Thus the ageing properties, i.e. the resistance towards humidity, are comparable for the two fibres [17].

Previous studies have shown the influence of organic acids on the dissolution of stone wool fibres [18]. Also, the dissolution of minerals with compositions similar to stone wool fibres have been shown to be highly dependent on the type and concentration of organic acids [19 to 22], due to the varying ability to form complexes with the dissolving elements.

The present study investigates the in-vitro dissolution behaviour of HT fibres compared to traditional stone wool fibres at pH 4.5 with the aim of clarifying the reason for the much higher dissolution rate of the HT fibres. The experimental work studied the effect of the various constituents in the synthetic simulated lung fluid while measuring the dissolution of silicon and aluminium, observing the formation of surface layers and determining the diameter decrease with time. The importance of the complex-forming ability of the organic acids and the effect of NaCl for the formation of surface layers is discussed.

2. Materials and methods

2.1 Study design

The in-vitro dissolution behaviour of the HT fibre and the traditional stone wool fibre (MMVF21) was investigated using a modified Gamble's solution [16], which is a synthetic simulated lung fluid.

The experimental work studied:

- the effect on the dissolution behaviour when removing individual components (e.g. phosphate, sodium chloride, organic acids) from Gamble's solution;
- the effect on the dissolution behaviour of the individual constituents present in Gamble's solution.

2.2 Test fibres: HT and MMVF21 fibres

Table 1 shows the chemical composition of the fibres used in the investigation. The fibres were produced by a cascade spinning process, with no addition of oil and binder. For practical reasons two batches of fibres were produced and used for the experiments.

2.3 Synthetic lung fluid (Gamble's solution)

The chemical composition of the modified Gamble's solution is shown in table 2.

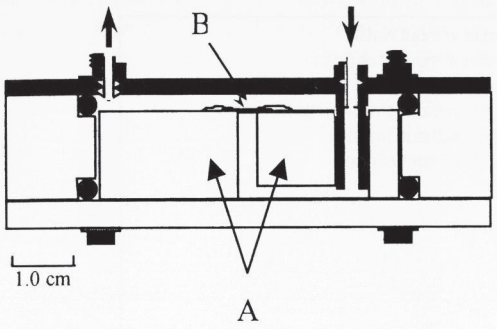

Figure 1. A cross-sectional view of the optical flow cell; A = mount on which the fibres = B were glued across.

2.4 Dissolution setup

The two methods used in the study to investigate the dissolution behaviour of HT and MMVF21 fibres were a stationary and an optical flow dissolution setup, respectively. All experimental work was performed at (37 ± 1) °C.

2.4.1 Stationary dissolution setup

The stationary dissolution setup comprised a container in which 300 mg fibres were mixed with 500 ml liquid (e.g. Gamble's solution) and continuously stirred. pH was kept at 4.5 (within ± 0.1) by adding 0.5 mol/l HCl using a Radiometer PMH290 pH-STAT controller connected to an ABU901 autoburette. A computer continuously recorded the amount of HCl added. Samples were taken at predetermined intervals and analysed for content of dissolved silicon and aluminium. All concentrations were given in mmol/l. Each experiment was carried out twice (average values used) except for the experiments with sodium + citrate.

This method revealed detailed information about the effect of the fluid on the dissolution behaviour (by measuring the amount of SiO_2 and Al_2O_3 dissolved).

2.4.2 Optical flow dissolution setup

The optical flow dissolution setup was developed by Potter [23], and comprised a flow cell in which individual fibres (typically 6 to 8 fibres) were fixed across a slot, through which the liquid (e.g. Gamble's solution) was pumped at a constant rate of 0.3 ml/min (figure 1). The liquid was kept at a constant pH of 4.5 ± 0.5. The dissolution rate (in ng/(cm^{2}h)) was calculated directly from the reduction in fibre diameter over time. See [23] for further details about the method.

With this method it was possible to measure the dissolution rate at well defined experimental conditions (e.g. no increase in pH, no saturation effects, etc.).

2.5 Scanning electron microscope

For visualization of the possible morphology changes of partly dissolved fibres, a Scanning Electron Microscope (SEM, Cambridge Stereoscan 360) was used. Furthermore, selected fibres from the two dissolution setups were EDX (Energy Dispersive Spectroscopy)-analysed to determine their chemical composition. The fibres were placed on double-faced carbon-tape and either gold (SEM)- or carbon (EDX)-coated prior to being measured.

3. Results

The influence of individual components in Gamble's solution on the dissolution of HT and traditional (MMVF21) stone wool fibres at pH 4.5 was investigated by excluding individual components from Gamble's solution (e.g. organic acids, phosphate and sodium chloride, respectively).

The results of both the stationary and optical setup (figures 2a and b and table 3) showed that citrate, sodium chloride and phosphate were the main components influencing the dissolution behaviour of HT and MMVF21 fibres. The absence of sodium chloride and phosphate resulted in a significantly higher dissolution rate, whereas the absence of citrate (and partly also tartrate) resulted in a significantly lower dissolution rate of HT and MMVF21 fibres at pH 4.5, comparable to the dissolution rate in Gamble's solution at pH 7.4.

The effect of the citrate concentration on the dissolution of HT and MMVF21 fibres was further investigated using the stationary setup. It was also investigated whether the effect of citrate was due to its buffer properties (pK_a = 4.7), meaning the ability of citrate to maintain a constant pH (pH 4.5) at the mineral surface. Acetate was used for comparison due to its similar buffer properties (pK_a = 4.7).

The results (figures 3a and b) showed that a doubling of the citrate concentration only caused a minor increase in dissolved aluminium and silicon for the MMVF21 fibre, whereas for HT fibres it doubled the amount of dissolved aluminium within the first 4 h. The amount of dissolved silicon increased by 60 %. The presence of acetate caused no (or only a moderate) dissolution of HT fibres.

The effect of citrate in combination with phosphate and sodium chloride was investigated in order to clarify the interaction between these components on the dissolution behaviour of HT and MMVF21 fibres (figures 4a and b and 5a and b).

A rather abrupt transition in the amount of dissolved silicon and aluminium was observed for the MMVF21 fibres, when the concentration of sodium chloride increased from 68 to 94 mmol/l (figures 5a and b). The

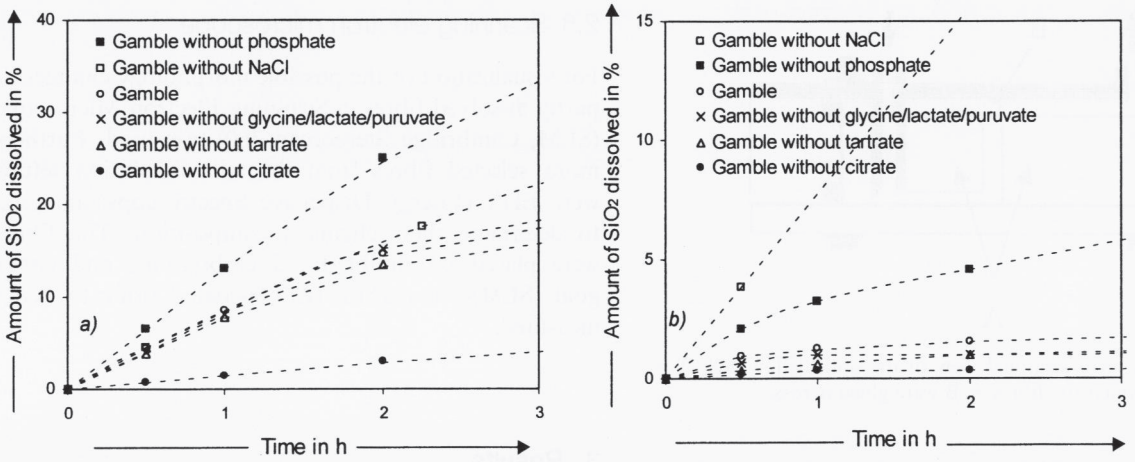

Figures 2a and b. Effect of excluding individual components from Gamble's solution on the dissolution behaviour of HT fibre (figure a) and MMVF21 fibre (figure b). Stationary setup, pH 4.5 and 37 °C.

Table 3. Calculated dissolution rate from the optical flow setup at pH 4.5 and 37 °C. Published results from similar measurements at pH 7.4 [23] are included for comparison.

	dissolution rate in 10^3 ng/(cm^{2}h)	
solution	HT fibre (r^2)	MMVF21 fibre (r^2)
Gamble	28.0 (0.992)	1.4 (0.839)
Gamble without phosphate	41.2 (0.990)	1.4 (0.640)
Gamble without sodium chloride	63.6 (0.996)	40.0 (0.993)
Gamble without organic acids	0.7 (0.999)	0.2 (0.974)
citrate	42.4 (0.884)	116.7 (0.977)
Gamble – pH 7.4	≈1	≈1

Note: r = regression coefficient.

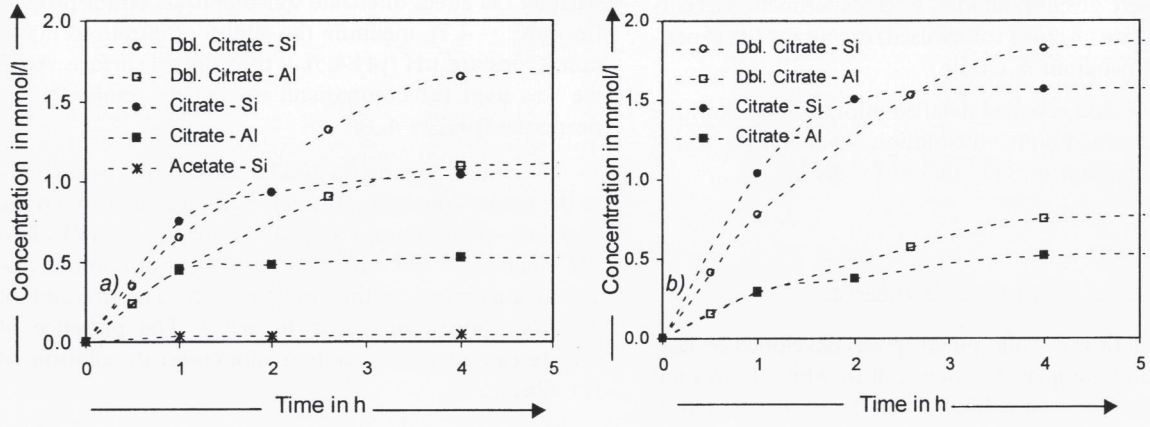

Figures 3a and b. Effect of citrate and acetate on the dissolution rate of HT fibre (figure a) and MMVF21 fibre (figure b). [citrate] = [acetate] = 0.52 mmol/l. Stationary setup, pH 4.5 and 37 °C.

presence of sodium chloride had no effect on the amount of dissolved silicon and aluminium at low concentrations ([NaCl] ≤ 68 mmol/l), but reduced the amount by 40 to 50 % at high concentrations (up to 122 mmol/l, corresponding to the sodium chloride concentration in the modified Gamble's solution). The addition of phosphate (results not shown) had no (or minor) effect when sodium chloride was not present.

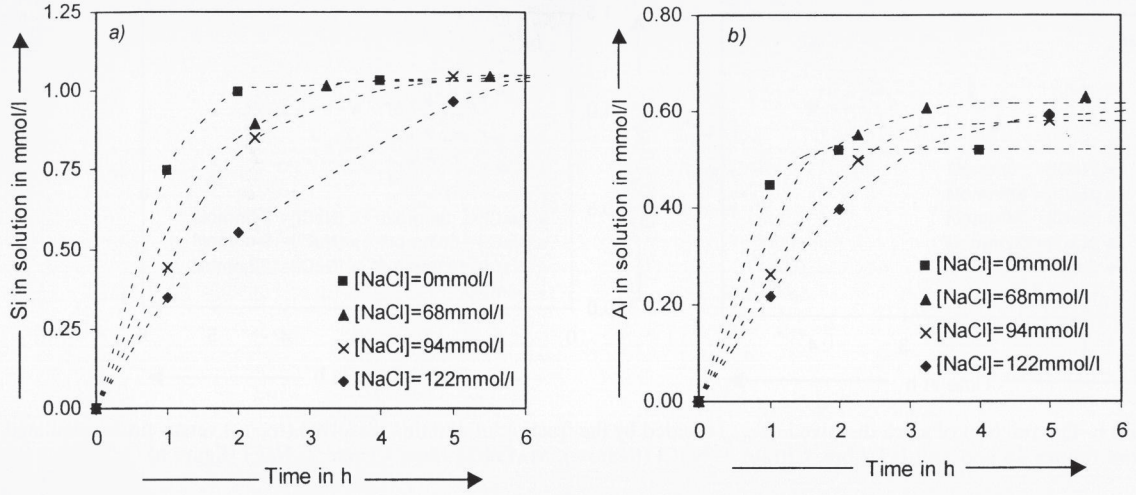

Figures 4a and b. Effect of sodium chloride in combination with citrate on the dissolution of HT fibres; determined by Si in solution (figure a) and Al in solution (figure b). Stationary setup, pH 4.5 and 37 °C. Citrate ([citrate] = 0.52 mmol/l) with increasing amounts of sodium chloride added ([NaCl] = 0–122 mmol/l).

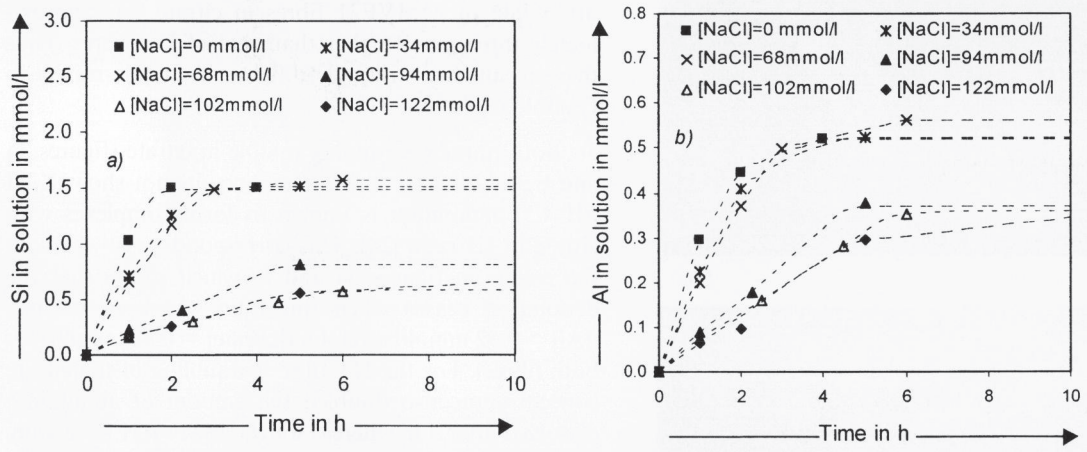

Figures 5a and b. Effect of sodium chloride in combination with citrate on the dissolution of MMVF21 fibres; determined by Si in solution (figure a) and Al in solution (figure b). Stationary setup, pH 4.5 and 37 °C. Citrate ([citrate] = 0.52 mmol/l) with increasing amounts of sodium chloride added ([NaCl] = 0–122 mmol/l).

However, when sodium chloride was present, the addition of phosphate made the transition less pronounced, and the amount of dissolved silicon and aluminium decreased with increasing concentrations of sodium chloride.

For the HT fibres (figures 4a and b), varying concentrations of sodium chloride had no effect on the total amount of dissolved silicon and aluminium, but the dissolution rate decreased with increasing concentrations of sodium chloride. No transition was observed.

Figures 6a and b show the fraction of silica dissolved (α_{SiO_2}) divided by the fraction of alumina dissolved ($\alpha_{Al_2O_3}$) (calculated from data from figures 4a and b and 5a and b). It is seen that the abrupt transition observed for MMVF21 exposed to citrate/sodium chloride is linked with a change from a silica depleted ($\alpha_{SiO_2}/\alpha_{Al_2O_3} > 1$) to a silica-enriched surface ($\alpha_{SiO_2}/\alpha_{Al_2O_3} < 1$). No similar change was observed for HT fibres.

SEM/EDX investigations of MMVF21 fibres exposed to citrate/sodium chloride or citrate/phosphate/sodium chloride revealed the formation of fairly thick surface layers (figure 7). The layers seemed quite porous and cracks were formed during drying. The surface layers apparently became denser as the sodium concentration increased, and the addition of phosphate caused a further densification. EDX analysis showed that phosphate was adsorbed onto these layers (3 to 7 wt% P_2O_5), and that the layers were enriched in silica at high sodium concentrations ([NaCl] ≥ 94 mmol/l). No layers were observed on HT fibres.

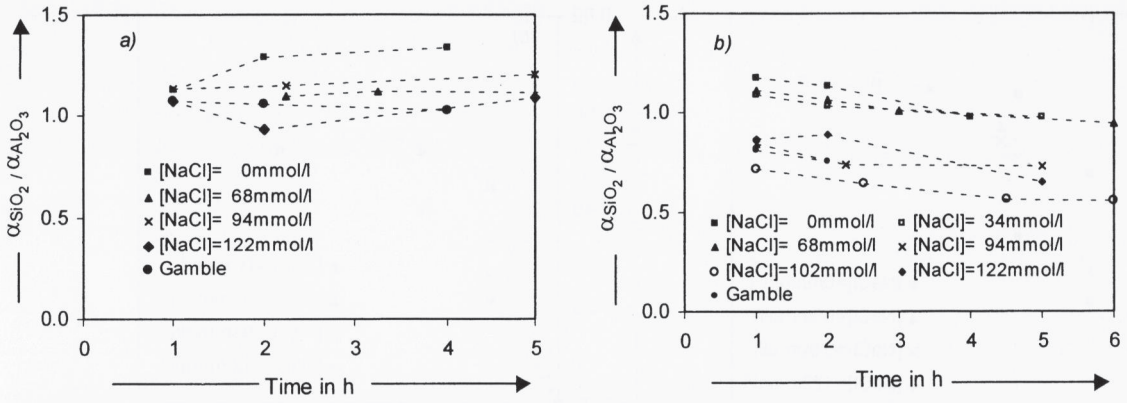

Figures 6a and b. The fraction of silica dissolved (α_{SiO_2}) divided by the fraction of alumina dissolved ($\alpha_{Al_2O_3}$) versus time (calculated from data from figures 4b and 5b); HT fibre: Citrate + NaCl (figure a), MMVF21 fibre: Citrate + NaCl (figure b).

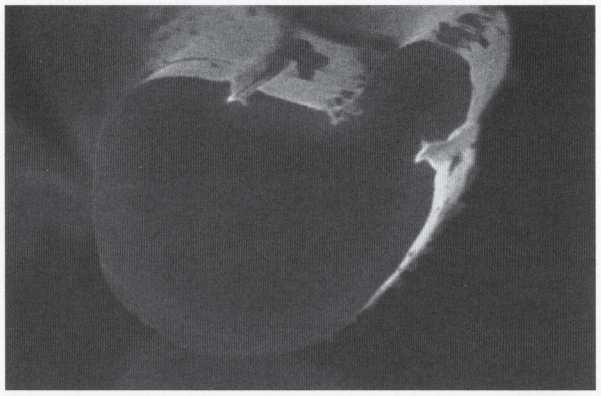

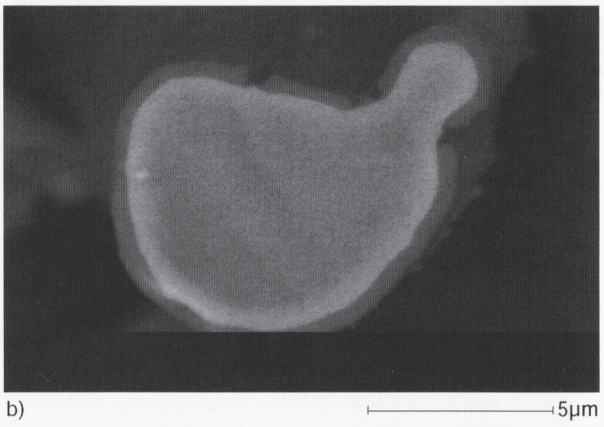

Figures 7a and b. SEM pictures of a MMVF21 fibre exposed to citrate + phosphate + 34 mmol/l NaCl; secondary image (sensitive to surface contour) (figure a), backscatter image (sensitive to atomic density variations) (figure b).

4. Discussion

The results with the various modifications of Gamble's solution (figures 2a and b and table 3) show that the dissolution rate depends strongly on the chemical composition of Gamble's solution. The absence of sodium chloride from Gamble's solution caused a significant increase in the dissolution rate of especially MMVF21 fibres (≈28 times) and a slight increase for HT fibres (≈2 times), resulting in comparable dissolution rates for HT and MMVF21 fibres in this solution. The dissolution rate of MMVF21 fibres in citrate was approximately three times higher than that of HT fibres. Thus these results are strikingly different from the results in Gamble's solution.

Both fibres were highly soluble in citrate (figures 3a and b and table 3) and tartrate (results not shown). At pH 4.5, aluminium is known to form complexes with citrate in 1:1 ratio [24]. This corresponds very well with the results in figures 3a and b, which shows that the dissolution ceases when this ratio has been reached ([Al] = 0.52 mmol/l after 4 h ([citrate] = 0.52 mmol/l) for both fibres). For the HT fibre, a doubling of the citrate concentration also doubled the amount of aluminium dissolved after 4 h, whereas for the MMVF21 fibre, only a minor increase in the amount of aluminium dissolved was observed, possibly due to saturation effects with respect to silica.

The observation that both fibres were highly soluble in citrate (figures 3a and b and table 3) and tartrate (results not shown) is in good agreement with a number of studies that have investigated the weathering of aluminium silicates in the presence of organic compounds at acidic pH. It has been shown that especially polyvalent hydroxy acids cause a significant increase in the dissolution rate [19 to 22]. This effect is due to the ability of hydroxy acids to form complexes (ligands) with aluminium. In weathering of alumina silicate minerals the dissolution rate is often modelled as [25]:

$$R_{tot} = R_H + R_L \quad (1)$$

where R_{tot} is the net dissolution rate observed, R_H is the proton-promoted dissolution rate, and R_L is the ligand-promoted dissolution rate. In case of minerals the ligand-promoted dissolution is believed to involve adsorption of ligands onto surface sites and subsequent release

of cations to the solution. The ligand-promoted dissolution has been shown to depend strongly on the Al/(Al+Si) ratio (increasing dissolution rate with increasing Al/(Al+Si) ratio) [19 and 26].

Acetic acid is not able to form complexes with aluminium, and the results from the comparison between citrate and acetate (figures 3a and b) showed that the buffer properties (proton-promoted dissolution) have insignificant impact on the dissolution rate as compared with the ability to form complexes (ligand-promoted dissolution) with aluminium. This means that the dissolution of HT and MMVF21 fibres at pH 4.5 is mainly ligand-promoted, and it thus explains why previous investigations [12 and 18] have found the measured in-vitro dissolution rate to be sensitive to the experimental conditions (i.e. citrate concentration and flow rate).

The addition of sodium chloride to the citrate solution (figures 4a and b and 5a and b) caused a radical change in the dissolution behaviour of MMVF21 fibres, whereas the dissolution behaviour of HT fibres remained relatively unaffected. Figures 6a and b demonstrate that the abrupt transition is linked with a change in the dissolution behaviour of the fibre (from a silica-depleted ($\alpha_{SiO_2}/\alpha_{Al_2O_3} > 1$) to a silica-enriched surface ($\alpha_{SiO_2}/\alpha_{Al_2O_3} < 1$)). The results from the optical flow dissolution setup (table 3) confirm that the presence (or absence) of sodium chloride has a major impact on the dissolution rate. The dissolution behaviour of both fibres in citrate + sodium chloride ([NaCl] > 68 mmol/l) resembles the dissolution behaviour observed in Gamble's solution ([NaCl] = 122 mmol/l) with respect to $\alpha_{SiO_2}/\alpha_{Al_2O_3}$.

The presence of sodium chloride is reported to decrease the dissolution rate of aluminium silicate minerals and silicates in general at acidic pH. Stillings and Brantley [27] studied the effect of sodium chloride on feldspar (aluminium silicate) dissolution rates and hypothesized that the decrease in dissolution rate with increasing sodium chloride concentration was due to competition between Na^+ and H^+ for adsorption on feldspar cation exchange sites. Schweda [28] hypothesized that the presence of sodium chloride resulted in a porous layer on the dissolving feldspar surface, which reduced the transport of protons to the surface, and thereby reduced the dissolution rate. A similar result is reported by Iler [29], who studied the formation of silica gels and their stability in the presence of sodium chloride. According to Iler the stability of the surface silica gel depends on the presence of sodium ions. The negatively charged sites at the surface of small silica gel particles may be neutralized by sodium ions, and thereby stabilize the gel. The negatively charged silica gel particles would otherwise turn into a sol and be transferred to the solution.

Our observations seem to be in line with the observations made by Iler, in the sense that stable silica-rich surface layers/gel are formed on MMVF21 fibres at sodium chloride concentrations similar to the concentration in the fluid (e.g. Gamble's solution) in the body (136 to 146 mmol/l) [30, 31]. The formation of such layers causes a significant diffusion barrier and ultimately protects the surface, limiting further dissolution. The chemical composition of the surface is in good agreement with the observed dissolution behaviour, the surface layers being enriched in SiO_2 at high sodium chloride concentrations.

A recent publication demonstrated a good correlation between Al/(Al+Si) ratio and the dissolution rate at pH 4.5 of a range of fibres, with an increasing dissolution rate with increasing Al/(Al+Si) ratio [32]. The observed difference in dissolution rate between HT and MMVF21 in Gamble's solution at pH 4.5 can reasonably be related to the Al/(Al+Si) ratio: the higher Al/(Al+Si) ratio for HT fibres results in a significantly different dissolution behaviour (as compared with MMVF21) due to the absence of stable silica-enriched surface layers. Other studies [19 and 21] have also found the dissolution rate at acidic conditions to increase when going from albite (resembles MMVF21 with respect to Al/(Al+Si) ratio) to anorthite (resembles HT with respect to Al/(Al+Si) ratio). The Al/(Al+Si) ratio for albite, anorthite, MMVF21 and HT is 0.25, 0.50, 0.25 and 0.40, respectively.

The aluminium in both fibres is in a tetrahedral co-ordination with a strong preference for co-ordination to silicon tetrahedrons [33]. This means that an increase in Al/(Al+Si) ratio results in a more hydrated and less continuous remaining silica network as aluminium is removed from the glass by citrate (and tartrate) present in Gamble's solution. This may reduce the ability to form dense surface layers and thereby result in a dissolution rate approximately ten times higher for HT as compared with MMVF21 fibres, which is believed to be the reason for the significantly increased biosolubility of the HT type of fibre [15].

5. Conclusion

The most important components in Gamble's solution at pH 4.5 for the dissolution of HT and MMVF21 fibres are the citrate and the sodium chloride. Citrate is able to form ligands with aluminium and thereby deplete the alumina-silica network of these ions, and sodium chloride is able to stabilize the remaining hydrated silica network. Therefore, when sodium chloride is not present in the solution, the remaining silica is readily dissolved.

The presence of sodium chloride lowers the dissolution rate, particularly the dissolution rate of MMVF21. Tentative suggestions explain this effect. The silica that remains when the silica network has been depleted of aluminium ions behaves differently. In HT fibres the silica dissolves at a high rate, probably as a diluted sol. In the MMVF21 fibres, condensation as a gel results in

a reduced dissolution rate. It is assumed that the different Al/(Al+Si) ratios of the HT and MMVF21 fibres explain why the fibres behave differently.

Our investigation shows that the dissolution behaviour of the MMVF21 fibres in Gamble's solution at pH 4.5 is significantly different from that of HT fibres. This means that the MMVF21 in Gamble's solution will dissolve at a lower rate, whereas the HT fibres will continue to dissolve at a high rate as the fluid is renewed. These dissolution characteristics are believed to explain the higher biosolubility of the HT fibres.

The fact that HT fibres have a moderate dissolution rate at neutral pH (pH 7.4) explains their resistance towards humidity (ageing), meaning that the fibres to a high degree maintain their initial properties after exposure to humidity. The ageing resistance being similar for HT and traditional stone wool fibres is of high importance for the application and practical use of the biosoluble HT fibres in all areas where previously traditional stone wool fibres were used.

*

Pia Nielsen and Birgit Jensen are acknowledged for their assistance with the experimental work.

6. References

[1] Davis, J. M. G.: Experimental data relating to the importance of fibre type, size, deposition, dissolution, and migration. In: Bignon, J.; Peto, J.; Saracci, R. (eds.): Non-occupational exposure to mineral fibres. Lyon: Int. Agency for Research on Cancer, 1989. p. 33–45. (IARC Scientific Publications No. 90).

[2] Oberdörster, G.: Deposition, elimination and effects of fibres in the respiratory tract of humans and animals. VDI Ber. **853** (1991) p. 17–37.

[3] Potter, R. M.; Mattson, S. M.: Glass fiber dissolution in a physiological saline solution. Glastechn. Ber. **64** (1991), no. 1, p. 16–28.

[4] Mattson, S.: Glass fibres in simulated lung fluid: Dissolution behaviour and analytical requirements. Ann. Occup. Hyg. **38** (1994) no. 6, p. 857–877.

[5] Thélohan, S.; Meringo, A. de: In vitro dynamic solubility test – influence of various parameters. Env. Health. Perspect. **102** (1994) suppl 5, p. 91–96.

[6] Zoitos, B.; Meringo, A. de; Rouyer, E. et al.: In vitro measurement of fiber dissolution rate relevant to biopersistence at neutral pH: An interlaboratory round robin. Inh. Tox. **9** (1997) p. 525–540.

[7] Bauer, J. F.; Law, B. L.; Hesterberg, T. W.: Dual pH durability studies of man-made vitreous fiber (MMVF). Environ. Health Perspect. **102** (1994) suppl 5, p. 61–66.

[8] Christensen, V. R.; Jensen, S. L.; Guldberg, M. et al.: Effect of chemical composition of man-made vitreous fibers on the rate of dissolution in vitro at different pHs. Env. Health Perspect. **102** (1994) suppl 5, p. 83–86.

[9] Guldberg, M.; Christensen, V. R.; Perander, M. et al.: Measurement of in-vitro fibre dissolution rate at acidic pH. Ann. Occup, Hyg. **42** (1997) no. 4, p. 223–243.

[10] Muhle, H.; Bellman, B.; Sebastian, K. et al.: Fasern – Tests zur Abschätzung der Biobeständigkeit und zum Verstaubungsverhalten. BIA-Report 2/98. Sankt Augustin: HVBG, 1998.

[11] Bernstein, D. M.; Morscheidt, C.; Grimm, H. et al.: Evaluation of soluble fibers using the inhalation biopersistence model, a nine-fiber comparison. Inh. Tox. **8** (1996) p. 345–385.

[12] Knudsen, T.; Guldberg, M.; Christensen, V. R. et al.: New type of stonewool (HT fibres) with a high dissolution rate at pH = 4.5. Glastech. Ber. Glass Sci. Technol. **69** (1996) no. 10, p. 331–337.

[13] Bellmann, B.; Muhle, H.; Kamstrup, O. et al.: Investigation on the durability of man-made vitreous fibres in rat lungs. Environ. Health Perspect. **102** (1994) suppl. 5, p. 185–189.

[14] Kamstrup, O.; Davis, J. M. G.; Ellehauge, A. et al.: The biopersistence and pathogenicity of man-made vitreous fibres after short- and long-term inhalation. Ann. Occup. Hyg. **42** (1998) no. 3, p. 191–199.

[15] Hesterberg, T. W.; Chase, G.; Axten, C. et al.: Biopersistence of synthetic vitrous fibres and amosite asbestos in rat lung inhalation. Toxicol. Appl. Pharmacol. **151** (1996) no. 2, p. 262–275.

[16] Test guideline for "In-vitro acellular dissolution of man-made vitreous silicate fibres at pH 4.5". Draft 11. EURIMA, 1998.

[17] Jensen, S. L.; Guldberg, M.; Christensen, V. R.: Ageing charecteristics of man made mineral fibres – accelerated tests under humid conditions. In: Fundamentals of Glass Science and Technology 1997. Proc. 4th Conf. Europ. Soc. Glass Sci. Technol. (ESG), Växjö 1997. Växjö: Glafo, 1997. p. 270–276.

[18] Mogensen, G.: The durability of mineral fibres in various buffer solutions. Riv. Stn. Sper. Vetro **5** (1984) no. 5, p. 135–138.

[19] Welch, S. A.; Ullman, W. J.: Feldspar dissolution in acidic and organic solutions: Compositional and pH dependence of dissolution rate. Geochim. Cosmochim. Acta **60** (1996) no. 16, p. 2939–2948.

[20] Lundström, U. S.: Significance of organic acids for weathering and the podzolization Process. Env. Int. **20** (1994) no. 1, p. 21–30.

[21] Welch, S. A.; Ullman, W. J.: The effect of organic acids on plagioclase dissolution rates and stoichiometry. Geochim. Cosmochim. Acta **57** (1993) p. 2725–2736.

[22] Stumm, W.: Catalysis of redox processes by hydrous oxide surfaces. CCACAA **70** (1997) no. 1, p. 71–93.

[23] Potter, R. M.: Method for determination of in-vitro fibre dissolution rate by direct optical measurement of diameter decrease. Glastech. Ber. Glass Sci. Technol. **73** (2000) no. 2, p. 46–55.

[24] Sposito, G. (ed.): The environmental chemistry of aluminum. 2nd. ed. Boca Raton, Fl: CRC Press, 1996.

[25] Amrhein, C.; Suarez, D. L.: The use of a surface complexation model to describe the kinetics of ligand-promoted dissolution of anorthite. Geochim. Cosmochim. Acta **52** (1988) p. 2785–2793.

[26] Stumm, W.; Furrer, G.: The dissolution of oxides and aluminum silicates; Examples of surface-coordination controlled kinetics. In: Stumm, W. (ed.): Aquatic surface chemistry. New York et al.: Wiley, 1987.

[27] Stillings, L. L.; Brantley, S. L.: Proton adsorption at the adularia feldspar surface. Geochim. Cosmochim. Acta **59** (1995) p. 1473–1482.

[28] Schweda, P.: Kinetics and mechanisms of alkali feldspar dissolution at low temperatures. Stockholm University, Ph. D. diss. 1990.

[29] Iler, R. K.: The chemistry of silica. Solubility, polymerization, colloid and surface properties, and biochemistry. New York Wiley, 1979.

[30] Nielson, D. W.: Electrolyte composition of pulmonary alveolar subphase in anaesthetised rabbits. J. Appl. Physiol. **60** (1986) no. 3, p. 972–979.

[31] Castranova, V.; Bowman, L.; Miles, P. R.: Transmembrane potential and ionic content of rat alveolar macrophages. J. Cell. Physiol. **101** (1979), p. 471–479.

[32] Guldberg, M.; Meringo, A. de; Kamstrup, O. et al.: The development of glass and stone wool compositions with increased biosolubility. Reg. Tox. Pharm. **32** (2000) p. 184–189.

[33] Lee, S. K.; Stebbins, J. F.: The degree of aluminum avoidance in aluminosilicate glasses. Am. Mineral. **84** (1999) p. 937–945.

0401P003

Address of the authors:

T. Steenberg, H. Kähler Hjenner,
S. L. Jensen, M. Guldberg, T. Knudsen
Rockwool International A/S
Hovedgaden 584
DK-2640 Hedehusene
e-mail: marianne.guldberg@rockwool.com